Improving PbS colloidal quantum dot solar cell performance via solution-phase engineering

Dhanvini Gudi[1], Arlene Chiu[1], Dana Kachman[1], Eric Rong[1], Serene Kamal[1], Yucheng Lan[2] Susanna M. Thon[1]

[1]Department of Electrical and Computer Engineering, Johns Hopkins University, Baltimore, Maryland, 21218, USA

[2]Department of Physics, Morgan State University, Baltimore, Maryland, 21218, USA

***Abstract* — Lead Sulfide (PbS) colloidal quantum dots (CQDs) are promising materials for flexible and wearable photovoltaic devices and technologies due to their low cost, solution processibility and bandgap tunability with quantum dot size. However, PbS CQD solar cells have limitations on performance efficiency due to charge transport losses in the CQD layers and hole transport layer (HTL). This study pursues two promising techniques in parallel to address these challenges. Solution-phase annealing of the absorbing PbS-PbX_2 (X = Br, I) layer can reduce charge transport losses by removing oleic acid and parasitic hydroxyl ligands. Additionally, optoelectronic simulations are used to show that HTL performance can be improved by the addition of a 2D transition metal dichalcogenide (TMD) layer to the PbS CQD-based HTL. We use solution-phase exfoliation to produce and incorporate 2D WSe_2 nanoflakes into the HTL. We report a power conversion efficiency (PCE) increase of up to 3.4% for the solution-phase-annealed devices and up to 1% for the 2D WSe_2 HTL augmented devices. A combination of these two techniques should result in high-performing PbS CQD solar cells, paving the way for further advancements in flexible photovoltaics.**

I. Introduction

Third generation photovoltaic research has lead to advancements in the development of novel materials that allow for higher efficiency while reducing processing costs. Lead Sulfide (PbS) colloidal quantum dots (CQDs) are one class of materials being investigated due to their properties such as low-cost solution processibility, size – bandgap tunability and infrared absorption [1], [2]. Owing to these beneficial properties, PbS CQDs are being explored for flexible and wearable photovoltaic device applications. Due to their solution processability, these materials can also be used with scalable manufacturing technologies reducing the processing costs further. The current standard PbS CQD solar cell device architecture is shown in Fig. 1a, where the illumination is through a transparent fluorine-doped tin oxide (FTO) coated glass substrate, on top of which a zinc oxide (ZnO) based electron transport layer (ETL) is deposited, followed by a solution-phase ligand exchanged PbS-PbX_2 (X = Br, I) absorbing layer, a PbS CQD hole transport layer (HTL) with ethanedithiol (EDT) ligands introduced during a solid-state exchange and top gold contacts [3].

While the advantages of PbS CQDs make them a promising candidate for flexible and wearable photovoltaic devices, PbS CQD solar cells have not been able to achieve efficiencies close to the theoretical limits, with a current record power conversion efficiency (PCE) for PbS CQD solar cells of 15.45%, demonstrated by Ding et. al. in 2022 [4]. The limited efficiencies have largely been attributed to non-radiative

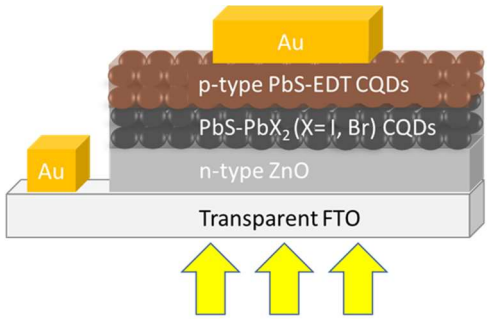

a.

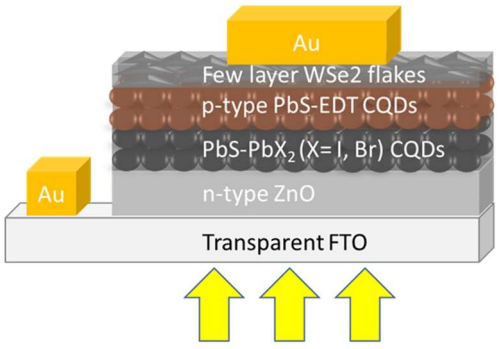

b.

recombination losses caused by poor charge transport within the CQD layer and carrier losses in the HTL [5], [6]. Therefore, improving the properties of PbS CQD films is an important problem to solve to push efficiencies forward.

Fig. 1. a. A standard PbS CQD solar cell device architecture. b. The device architecture with a WSe_2 HTL layer incorporated on the PbS-EDT HTL layer.

2023 IEEE 50th Photovoltaic Specialists Conference (PVSC) | 978-1-6654-6059-0/23/$31.00 ©2023 IEEE | DOI: 10.1109/PVSC48320.2023.10359532

This study takes a two-pronged approach to this problem. The first approach is improvement of the charge transport properties of the PbS-PbX_2 absorbing layer by solution-phase annealing of the ligand-exchanged absorbing layer material. This technique has been shown to improve charge transport within the absorbing layer by the thermal desorption of bulky oleic acid (OA^-) and parasitic OH^- ligands [7]. The second approach is augmentation of the existing PbS-EDT HTL layer by the addition of 2D transition metal dichalcogenide (TMD) nanoflakes to improve HTL charge mobility and carrier transport. Our previous compuational studies have predicted improved carrier mobility in the HTL with the addition of a few-layer-thick WSe_2 film onto the PbS–EDT layer[8]. This study involves experimental fabrication of solar cells with solution-exfoliated few-layer 2D WSe_2 on top of the PbS-EDT HTL as shown in Fig 1.b. We test the two approaches separately and measure the current density – voltage (J-V) profiles of the resulting solar cells to extract figures of merit and compare performances. We also optically characterize the few-layer 2D WSe_2 to study its properties. We hypothesize that combining these two approaches would greatly improve the performance of PbS CQD solar cells by addressing some of their challenges and paving the way for further advancements to reach theoretical efficiency limits.

II. EXPERIMENTS AND RESULTS

A. Solution phase anneal of ligand-exchanged absorbing layer

PbS-PbX_2 (X = Br, I) is synthesized by a solution-phase ligand exchange process that involves replacing oleic acid ligands on PbS CQDs with PbX_2. There is a need to remove OA^- and OH^- ligands from the ligand-exchanged solution as they can cause an electronic barrier to charge transport and unwanted carrier recombination, respectively. The solution-phase ligand exchange is performed by following standard procedures in which oleic acid capped PbS CQDs are added to PbX_2 in dimethylformamide and vortexed until solvent separation is observed[9]. Next, the solution is washed with octane three times and annealed for 1 hour, after which it is dispersed in a solution composed of butylamine, pentalyamine and hexylamine. In this work, we optimize a solution-phase annealing procedure to maximize device PCE.

TABLE I
SUMMARY OF DEVICE PERFORMANCE FOR DIFFERENT SOLUTION-ANNEAL TEMPERATURES

Device	PCE [%] best, (average)	Voc [V] best, (average)	Jsc [mA/cm^2] best, (average)	Fill Factor best, (average)
Control	6.9, (5.9±0.7)	0.61, (0.59±0.01)	22.5, (19.4±1.8)	0.47, (0.42±0.04)
50°C solution annealed	8.2, (7.1±0.7)	0.58, (0.57±0.01)	24.4, (21.9±1.8)	0.47, (0.47±0.02)
60°C solution annealed	8.9, (7.5±2.1)	0.57, (0.57±0.01)	28.3, (24.2±2.4)	0.45, (0.48±0.04)
70°C solution annealed	10.3, (9.1±0.7)	0.56, (0.56±0.01)	28.4, (27.2±1.9)	0.54, (0.49±0.03)

We chose three anneal temperatures – 50°C, 60°C and 70°C based on literature and experimental observations [7], [10], [11]. We varied the anneal time periods from 30 minutes to 1.5 hours, and found 1 hour to be the optimized period. Shorter anneal times did not show much change from the control performance whereas longer anneal times caused degradation of the absorbing layer material. The temperature dependent studies are summarized in Table 1. From the table, it can be seen that compared to the control device with no solution-phase anneal, the device with a 70°C solution-phase anneal exhibited the highest increase in PCE by 3.4%. These findings demonstrate that this technique significantly improves device performance with a noted increase in the Jsc, indicating that there is a high likelihood of oleic acid ligands being desorbed from the PbS-PbX_2, thereby improving charge transport in the active layer.

B. 2D WSe_2 as a HTL additive for PbS CQD solar cells

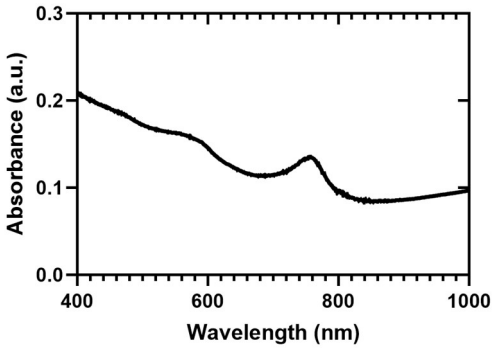

Fig. 2. Absorption spectrum of few-layer solution-phase exfoliated WSe_2 nanoflakes .

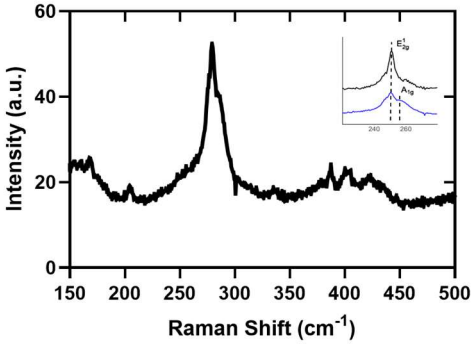

Fig. 3. Raman spectrum of few-layer solution-phase exfoliated WSe_2 nanoflakes with a prominent E_{2G} peak at 250 cm^{-1} . Inset shows the E_{2G} peak at 250 cm^{-1} and a shoulder A_{1G} peak at 257 cm^{-1} for 2D nanoflake WSe_2 (blue) compared to bulk WSe_2 (black) with no A_{1G} peak.

Following previous investigations from our group using 1-D SCAPS [12] to model the effect of WSe_2 as a HTL in PbS CQD solar cells, solution-processed WSe_2 nanoflakes were produced, characterized and incorporated into PbS CQD solar cells to study their impact on device performance [8]. We performed solution-phase exfoliation of commercial bulk WSe_2 powder in ethanol using probe sonication to obtain 2D WSe_2 nanoflakes. These flakes were spin-cast onto the PbS-EDT layer of the solar cell at different spin speeds to study coverage and device performance. Optical characterization of the-few layer 2D WSe_2 was performed using UV-Visible-Near-Infrared spectrophotometry (UV-Vis-NIR) to study absorption as shown in Fig. 2, and Raman spectroscopy was performed as shown in Fig. 3 to qualitatively determine if the films were bulk-like or a few layers thick. From Fig. 2 we can observe an onset absorption peak at 750 nm, consistent with literature [13]. From the Raman spectroscopy (Fig. 3 inset), we observed that bulk WSe_2 powder (black) only showed the dominant 250 cm^{-1} characteristic E_{2G} peak whereas the solution-phase exfoliated film (blue) also showed a shoulder A_{1G} peak at 257 cm^{-1}, characteristic of a few-monolayer-thick film [13]–[15].

The solution-phase exfoliated 2D WSe_2 nanoflakes were spin-cast after the HTL on standard devices at different speeds as listed in Table II. It can be seen that WSe_2 spin-cast at 1000 rpm offered the highest increase in PCE of 1% compared to the control. Scanning electron microscopy (SEM) measurements suggest that this was likely due to slower spin speeds (500 rpm) causing aggregation of flakes and non uniformity of the HTL layer, whereas higher spin speeds enabled more uniform coverage. It is important to note that the control devices reported in Tables I and II differed slightly in performance due to slight differences in processing conditions and materials.

TABLE II
SUMMARY OF DEVICE PERFORMANCE FOR DIFFERENT SPIN SPEEDS OF SOLUTION-PROCESSED WSE_2 FILMS

Device	PCE [%] best, (average)	Voc [V] best, (average)	Jsc [mA/cm^2] best, (average)	FF best, (average)
Control	8.7, (7.3±0.7)	0.65, (0.61±0.02)	24.0, (23.5±1.5)	0.56, (0.50±0.04)
WSe_2 spun at 2000 rpm	9.5, (7.9±0.8)	0.63, (0.60±0.03)	26.0, (23.6±1.7)	0.58, (0.55±0.03)
WSe_2 spun at 1000 rpm	9.7, (8.4±1.2)	0.58, (0.62±0.04)	27.8, (23.7±2.7)	0.60, (0.54±0.04)
WSe_2 spun at 500 rpm	9.4, (8.0±1.0)	0.62, (0.62±0.03)	25.9, (23.8±2.2)	0.59, (0.50±0.03)

III. CONCLUSIONS AND SUMMARY

This study experimentally verified two promising techniques to improve PbS CQD solar cell device performance, with a PCE increase of up to 3.4% obtained by solution-phase annealing of the PbS-PbX_2 layer and a PCE improvement of up to 1% obtained by integration of a few-layer 2D WSe_2 HTL. Future steps include combining these two techniques to test and validate the performance improvement of devices and further characterization of material and optical properties. This study aimed to improve the performance of PbS CQD solar cells and allow for further innovation in next generation solar cell technologies.

IV. ACKNOWLEDGEMENTS

National Science Foundation (DMR-1807342) and US Department of Defense (W911NF2120213) for funding. Prof. Natalia Drichko for Raman Spectroscopy.

REFERENCES

[1] S. Malhotra, L. Gupta, R. Pandey, and R. Sharma, "A critical review on the recent progress in the area of PbS CQDs based solar cell technology," 2022, p. 020016. doi: 10.1063/5.0110868.

[2] M. Yuan *et al.*, "Phase-Transfer Exchange Lead Chalcogenide Colloidal Quantum Dots: Ink Preparation, Film Assembly, and Solar Cell Construction," *Small*, vol. 18, no. 2, p. 2102340, Jan. 2022, doi: 10.1002/smll.202102340.

[3] A. Chiu, C. Bambini, E. Rong, Y. Lin, and S. M. Thon, "New Hole Transport Materials via Stoichiometry-Tuning for Colloidal Quantum Dot Photovoltaics," in *2020 47th IEEE Photovoltaic Specialists Conference (PVSC)*, Jun. 2020, pp. 1096–1097. doi: 10.1109/PVSC45281.2020.9300891.

[4] C. Ding *et al.*, "Over 15% Efficiency PbS Quantum-Dot Solar Cells by Synergistic Effects of Three Interface Engineering: Reducing Nonradiative Recombination and Balancing Charge Carrier Extraction," *Adv Energy Mater*, vol. 12, no. 35, p. 2201676, Sep. 2022, doi: 10.1002/aenm.202201676.

[5] S. Liu *et al.*, "Enhancing the Efficiency and Stability of PbS Quantum Dot Solar Cells through Engineering an Ultrathin NiO Nanocrystalline Interlayer," *ACS Appl Mater Interfaces*, vol. 12, no. 41, pp. 46239–46246, Oct. 2020, doi: 10.1021/acsami.0c14332.

[6] L. Hu *et al.*, "Optimizing Surface Chemistry of PbS Colloidal Quantum Dot for Highly Efficient and Stable Solar Cells via Chemical Binding," *Advanced Science*, vol. 8, no. 2, p. 2003138, Jan. 2021, doi: 10.1002/advs.202003138.

[7] X. Liu *et al.*, "Solution Annealing Induces Surface Chemical Reconstruction for High-Efficiency PbS Quantum Dot Solar Cells," *ACS Appl Mater Interfaces*, vol. 14, no. 12, pp. 14274–14283, Mar. 2022, doi: 10.1021/acsami.2c01196.

[8] E. Rong, A. Chiu, C. Bambini, Y. Lin, C. Lu, and S. M. Thon, "New Chalcogenide-Based Hole Transport Materials for Colloidal Quantum Dot Photovoltaics," in *2021 IEEE 48th Photovoltaic Specialists Conference (PVSC)*, Jun. 2021, pp. 0750–0753. doi: 10.1109/PVSC43889.2021.9518695.

[9] A. Chiu, E. Rong, C. Bambini, Y. Lin, C. Lu, and S. M. Thon, "Sulfur-Infused Hole Transport Materials to Overcome Performance-Limiting Transport in Colloidal Quantum Dot Solar Cells," *ACS Energy Lett*, vol. 5, no. 9, pp. 2897–2904, Sep. 2020, doi: 10.1021/acsenergylett.0c01586.

[10] Y. Shi *et al.*, "Influence of the Post-Synthesis Annealing on Device Performance of PbS Quantum Dot Photoconductive Detectors," *physica status solidi (a)*, Jul. 2018, doi: 10.1002/pssa.201800408.

[11] B. Ding, Y. Wang, P.-S. Huang, D. H. Waldeck, and J.-K. Lee, "Depleted Bulk Heterojunctions in Thermally Annealed PbS Quantum Dot Solar Cells," *The Journal of Physical Chemistry C*, vol. 118, no. 27, pp. 14749–14758, Jul. 2014, doi: 10.1021/jp502356d.

[12] M. Burgelman, P. Nollet, and S. Degrave, "Modelling polycrystalline semiconductor solar cells," *Thin Solid Films*, vol. 361–362, pp. 527–532, Feb. 2000, doi: 10.1016/S0040-6090(99)00825-1.

[13] W. Zhao *et al.*, "Evolution of Electronic Structure in Atomically Thin Sheets of WS2 and WSe2," *ACS Nano*, vol. 7, no. 1, pp. 791–797, Jan. 2013, doi: 10.1021/nn305275h.

[14] A. Arora, M. Koperski, K. Nogajewski, J. Marcus, C. Faugeras, and M. Potemski, "Excitonic resonances in thin films of WSe2 : from monolayer to bulk material," *Nanoscale*, vol. 7, no. 23, pp. 10421–10429, 2015, doi: 10.1039/C5NR01536G.

[15] Q. Cui, F. Ceballos, N. Kumar, and H. Zhao, "Transient Absorption Microscopy of Monolayer and Bulk WSe2," *ACS Nano*, vol. 8, no. 3, pp. 2970–2976, Mar. 2014, doi: 10.1021/nn500277y.